A LARGE-SCALE SHOCK SURROUNDING A POWERFUL RADIO GALAXY

J. H. CROSTON[1], M. J. HARDCASTLE[2], B. MINGO[2], D. A. EVANS[3,4], D. DICKEN[5], R. MORGANTI[6,7], C. N. TADHUNTER[8]
Draft version December 1, 2010

ABSTRACT

We report the *Chandra* detection of a large-scale shock, on scales of 200 kpc, in the cluster surrounding the powerful radio galaxy 3C 444 (PKS 2211−17). Our 20-ks *Chandra* observation allows us to identify a clear surface brightness drop around the outer edge of the radio galaxy, which is likely to correspond to a spheroidal shock propagating into the intracluster medium. We measure a temperature jump across the surface brightness drop of a factor ~ 1.7, which corresponds to a Mach number of ~ 1.7. This is likely to be an underestimate due to the need to average over a fairly large region when measuring the temperature of the post-shock gas. We also detect clear cavities corresponding to the positions of the radio lobes, which is only the second such detection associated with an FRII radio galaxy. We estimate that the total energy transferred to the environment is at least 8.2×10^{60} ergs, corresponding to a jet power of $> 2.2 \times 10^{45}$ ergs s^{-1} (assuming a timescale based on the measured shock speed). We also compare the external pressure acting on the lobes with the internal pressure under various assumptions, and conclude that a significant contribution from protons is required.

1. INTRODUCTION

The presence of large-scale shocks surrounding powerful radio galaxies has long been a prediction from models of their evolution (e.g. Scheuer 1974; Kaiser & Alexander 1997), and it was realised prior to the launch of the *Chandra* X-ray observatory that such shocks in radio-galaxy environments should be detectable with our current generation of X-ray instruments (e.g. Heinz, Reynolds & Begelman 1998). Deep *Chandra* observations have now firmly identified weak shocks in the intracluster medium surrounding nearby low-power [FRI: Fanaroff & Riley (1974) class 1] sources, such as Perseus, Hydra A, and M87 (e.g. Fabian et al. 2003; Nulsen et al. 2005a; Forman et al. 2007), and a few examples of strong shocks have been found surrounding smaller sources (e.g. Kraft et al. 2003; Croston et al. 2007; Croston et al. 2009).

Recent work investigating radio galaxy impact with large samples (e.g. Dunn et al. 2008; Bîrzan et al. 2008; Cavagnolo et al. 2010) has also tended to focus on lower power objects, for two major reasons. Firstly their role as a means of feedback in galaxy evolution is currently perceived to be more important, due to their higher number density and ubiquity at the centers of "cool-core" clusters (e.g. Cavagnolo et al. 2008). In addition, most X-ray cavity and weak shock detections reported in the literature are associated with FRI radio galaxies, due mainly to the relative scarcity of FRIIs in the nearby clusters where cavities and shocks can easily be detected, but also perhaps partly due to the presence of X-ray inverse-Compton emission which dominates over thermal emission from the ICM for many nearby FRII radio galaxies in poorer environments (e.g. Croston et al. 2005; Kataoka & Stawarz 2005).

Shocks surrounding powerful FRII radio galaxies have so far proved somewhat elusive, although there is evidence for a large-scale shock surrounding Cygnus A (Smith et al. 2002), as well as a weak shock surrounding the intermediate FRI/II radio galaxy Hercules A (Nulsen et al. 2005b). The investigation of shocks around FRII radio galaxies is important, however, as they could play a role in galaxy feedback at high redshift (e.g. Rawlings & Jarvis 2004). Detections of shocks and cavities associated with FRII radio galaxies offer an independent means of investigating the conclusions of inverse-Compton and environmental studies, which suggest that in most cases FRII radio galaxies are close to equipartition between radiating particles and magnetic field, and do not require a significant proton population for pressure balance (e.g. Croston et al. 2005, Kataoka & Stawarz 2005), in contrast to the FRI population (e.g. Croston et al. 2008a). A few FRIIs in rich cluster environments appear to deviate from this conclusion (e.g. Belsole et al. 2007; Hardcastle & Croston 2010), which might indicate a relationship between particle content and environment. It is important to establish whether such a relationship exists in order to account correctly for the energetics of different radio-galaxy populations within galaxy feedback models.

Here we report the detection of a large-scale shock surrounding the weak-lined FR II radio galaxy 3C 444 ($z = 0.153$, $L_{1.4GHz} = 3.3 \times 10^{26}$ W Hz^{-1}), which is found at the center of the cluster Abell 3847 ($L_X \sim 10^{44}$ erg s^{-1} – see below), and present an investigation of its dynamics and energetics. Throughout the paper we use a cosmology in which $H_0 = 70$ km s^{-1} Mpc^{-1}, $\Omega_{\rm m} = 0.3$ and $\Omega_\Lambda = 0.7$, corresponding to an angular scale of 2.66 kpc arcsec^{-1} at this redshift. Galactic absorption of $N_{\rm H} = 2.51 \times 10^{20}$ cm^{-2} is assumed for all X-ray spectral fits. Spectral indices α are defined in the sense $S_\nu \propto \nu^{-\alpha}$. Reported errors are 1σ for one interesting parameter, except where otherwise noted.

[1] School of Physics and Astronomy, University of Southampton, Southampton, SO17 1BJ, UK.; J.Croston@soton.ac.uk

[2] School of Physics, Astronomy and Mathematics, University of Hertfordshire, Hatfield, Hertfordshire, AL10 9AB, UK

[3] Harvard-Smithsonian Center for Astrophysics, 60 Garden Street, Cambridge, MA 02138, USA

[4] Elon University, Elon, NC 27244, USA

[5] Department of Physics and Astronomy, Rochester Institute of Technology, 84 Lomb Memorial Drive, Rochester, NY 14623, USA

[6] Netherlands Institute for Radio Astronomy, Postbus 2, 7990 AA, Dwingeloo

[7] Kapteyn Astronomical Institute, University of Groningen, P.O. Box 800, 9700 AV Groningen, The Netherlands

[8] Department of Physics and Astronomy, University of Sheffield, Sheffield S3 7RH

2. OBSERVATIONS AND DATA ANALYSIS

We observed 3C 444 (PKS 2211−17) with the *Chandra* ACIS-S detector for 20 ks on 2009 March 20th, as part of

a programme to complete observations of the southern 2Jy sample of radio galaxies (Tadhunter et al. 1993; Morganti et al. 1993). The observation was taken in VFAINT mode to minimize the background level. The data were reprocessed from the level 1 events file with CIAO 4.2 and CALDB 4.3, including VFAINT cleaning. The latest gain files were applied and the 0.5-pixel randomization removed using standard techniques detailed in the CIAO on-line documentation[9]. An inspection of the lightcurve for our observation using the *analyze_ltcrv* script showed that there were no periods of high background level, and so no additional GTI filtering was applied. The radio analysis in this paper is based on archival VLA observations at 1.4-GHz and 5 GHz (program ID AD276). The data were calibrated and imaged within AIPS in the standard manner.

We produced a $0.5 - 5$ keV filtered image from the *Chandra* data to examine the X-ray emission associated with the radio galaxy and environment, which is presented in Fig. 1. The relationship between the X-ray and radio emission is shown in Fig. 2. Extended emission associated with the surrounding galaxy cluster is clearly detected, with prominent cavities at the positions of the two radio lobes. We note that this is only the second detection of clear cavities associated with a radio galaxy that can be unambiguously classified as an FRII based on its morphology (narrow collimated jets and a compact hotspot in the northern lobe) and radio luminosity. The X-ray surface brightness also decreases noticeably beyond an elliptical region enclosing the radio galaxy.

We first extracted a global spectrum for the cluster (excluding the central $2''$ and the radio lobes to avoid non-thermal contamination) and fitted an APEC model to characterize its global properties. We measure a global temperature of $kT = 3.5 \pm 0.2$ keV, and a bolometric X-ray luminosity of 1.0×10^{44} erg s^{-1}, consistent with a moderately rich cluster and in line with observed $L_X - T_X$ relations (e.g Pratt et al. 2009). The overall X-ray morphology is very regular, apart from the X-ray cavities, and as reported later (Table 1 and Fig. 4) we do observe a moderate decrease in central temperature and peak in surface brightness; however, the central density based on extrapolating from a beta model fit to the inner regions is slightly lower than the value of $h(z)^{-2}n_{e,0} > 4 \times 10^{-2}$ cm^{-2} used to distinguish cool-core clusters by Pratt et al. (2009), hence it may not be a strong cool-core system.

In order to investigate whether the observed surface brightness decrease is associated with a shock, we extracted surface brightness profiles and spectra in several regions of interest. In particular we considered an elliptical region chosen to surround the bright X-ray emission, which we divided into three elliptical annuli. Two of the annuli were further subdivided into quadrants to investigate temperature structure. Our spectral extraction regions are indicated in Fig. 3. An elliptical annulus beyond the bright X-ray region was also used ("Outer region" in Table 1). Fig. 4 shows the surface brightness profiles in the N-S and E-W directions. In both directions the profile flattens in a way not typically seen in undistorted cluster profiles (e.g. Cavagnolo et al. 2009), and then drops steeply. The steepening is sharpest in the N-S direction, where there is an abrupt turn-over at a distance of ~ 45 arcsec, consistent with the edge of the X-ray bright region shown in Fig. 2. The location of the turn-over appears to be at the same distance from the nucleus in both the North and South direction.

Spectra for the eight annular quadrants as well as the in-
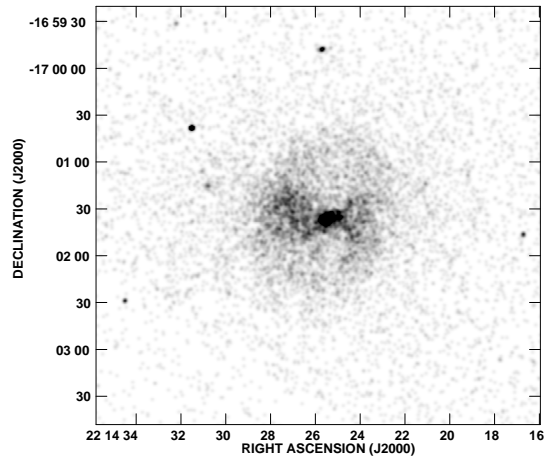

FIG. 1.— A 0.5 - 5.0 keV image of the *Chandra* data, lightly smoothed with a Gaussian kernel of $\sigma = 3$ pix.
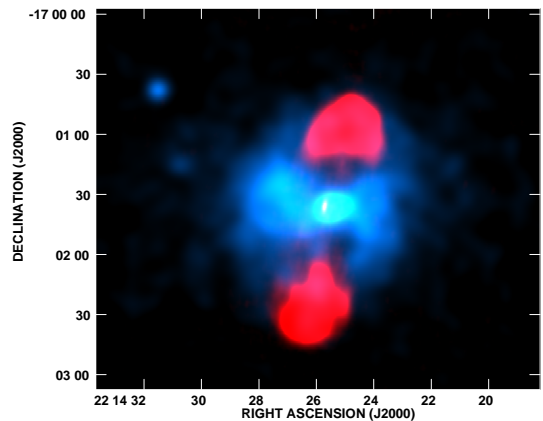

FIG. 2.— An image made from the *Chandra* data (shown in blue, smoothed with a Gaussian of $\sigma = 15$ pix) and the 5-GHz VLA map (shown in red), indicating the relationship between the radio and X-ray structures, including cavities at the position of the radio lobes, and a sharp elliptical surface brightness drop surrounding the source.

ner and outer regions were fitted with the APEC[10] model. The results of this spectral fitting are listed in Table 1. The abundance was poorly constrained in free abundance fits, and so we report the results of fits with abundance fixed at $0.3 \times$ solar abundance. A crude temperature map using the same regions is shown in Fig. 3. Spectral results for the AGN nucleus will be presented in Mingo et al. (in prep.). The nuclear count rate is insignificant compared to the emission from the cluster gas, and so is not a contaminating source of non-thermal emission for our analysis.

The results of spectral fitting to the radio lobe regions (extraction regions chosen to encompass the extent of radio emission) are listed in Table 1. It is clear from the detection of X-ray cavities in our *Chandra* data that any lobe inverse-Compton emission (cf. Croston et al. 2005) is weak relative to the cluster X-ray emission; however, it is important to be certain that non-thermal emission cannot be contaminating our spectral results. As shown in Table 1, a thermal model was a significantly better fit than a power-law model

---

[9] http://asc.harvard.edu/ciao/

[10] Astrophysical Plasmas Emission Code - http://cxc.harvard.edu/atomdb/

TABLE 1
RESULTS OF SPECTRAL MODELLING FOR CLUSTER GAS EMISSION AND RADIO LOBES[a]

Region	Subregion/Model	Temperature (keV)	Γ	χ^2	D.O.F.
Annulus 1		2.2 ± 0.2		36.5	39
Annulus 2	N	$4.0^{+0.7}_{-0.6}$		24.6	27
	E	$3.4^{+0.4}_{-0.3}$		28.8	39
	S	$4.8^{+1.1}_{-0.8}$		10.2	19
	W	$5.1^{1.1}_{-0.8}$		31.4	28
Annulus 3	N	$6.2^{+2.2}_{-1.3}$		11.3	19
	E	$2.9^{+0.6}_{-0.5}$		8.3	14
	S	$2.9^{+1.1}_{-0.6}$		1.2	6
	W	$3.8^{+1.6}_{-1.0}$		4.5	7
Outer region		$3.6^{+0.5}_{-0.4}$		58.8	62
Lobes	PL		1.78 ± 0.04	82.5	71
	APEC	3.91 ± 0.33		63.8	71
	PL + APEC[b]	3.7 ± 0.5	1.7^c	63.7	70

[a] All spectral fits are in the energy range $0.4 - 7$ keV, using an APEC model with abundance fixed at $0.3\times$ solar abundance.
[b] The 0.4 - 7.0 keV unabsorbed flux in was measured to be $< 3.1 \times 10^{13}$ ergs cm^{-2} s^{-1} and $(5.2^{+0.7}_{-1.8}) \times 10^{-13}$ ergs cm^{-2} s^{-1} for the PL and APEC components, respectively.
[c] The power-law photon index tended to very low values of ~ 0.3, and so we fixed its value at a physically reasonable value for lobe inverse-Compton emission so as to test the possible presence of such a component.
[d] The lower bound on the normalisation of the power-law component was consistent with zero.
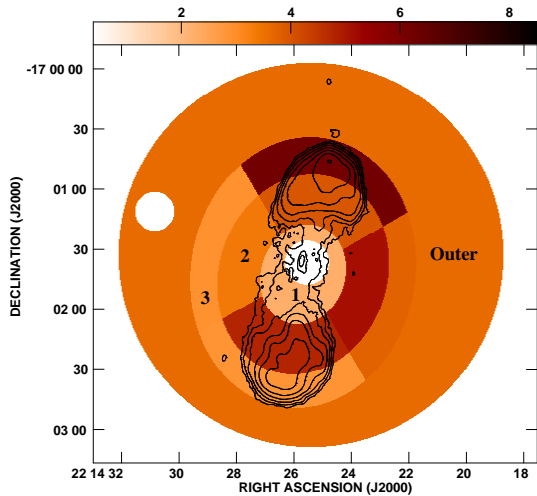

FIG. 3.— Temperature map (in keV) produced using the results of the spectral fits in Table 1 (regions as in Fig, 1), with 5-GHz contours overlaid. White regions do not have measured temperatures. The small circle to the east is a contaminating point source excluded from the fits. The regions used in Table 1 are indicated with annulus numbers/region names.
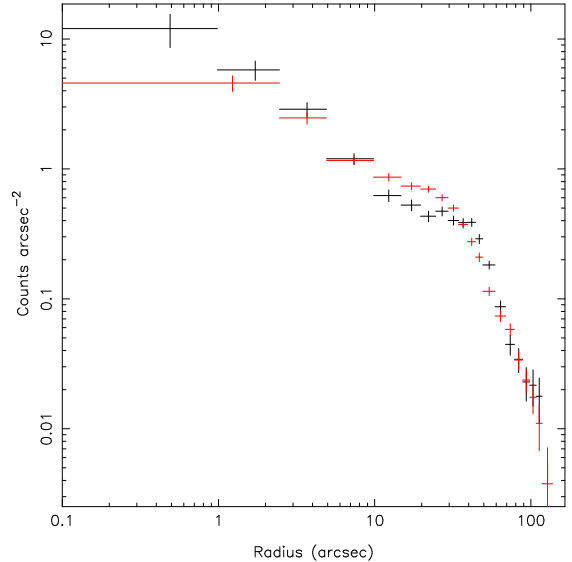

FIG. 4.— X-ray surface brightness profiles of the emission surrounding 3C 444. The emission was divided into 4 quadrants, with the North and South quadrants combined to make a longitudinal profile (black) and the East and West quandrants combined to make a transverse profile (red). A sharp drop is present in the N-S direction at ~ 45 arcsec, while a less sharp drop is present at ~ 30 arcsec in the E-W direction.

to the lobe regions; however, a thermal + power-law model also gave a good fit with a significant power-law contribution, corresponding to a 1-keV flux density of 9 nJy, which is a factor of ~ 4 higher than the IC prediction if the source was at equipartition [based on modelling using the code of Hardcastle et al. (1998)]. Such a departure from equipartition is consistent with the results for the FRII population (e.g. Croston et al. 2005); however, the presence of this spectral component is not formally required by the data, therefore we cannot consider this an inverse-Compton detection. Reassuringly, the temperature of the thermal component in the model is not significantly affected by the presence of a power-law contribution at this level. IC emission at a higher level is unlikely: our previous work on large samples of FRII radio galaxies has

shown that the level of lobe IC is narrowly distributed, with a mean level a factor 2–3 above the equipartition prediction. We therefore conclude that our temperature measurements are not affected by inverse-Compton contamination.

3. EVIDENCE FOR A SHOCK SURROUNDING 3C 444

As shown in Fig. 4, the surface brightness drops by a factor of ~ 10 between 45 and 70 arcsec from the AGN nucleus (or cluster center). This corresponds roughly to a density jump of a factor of ~ 3, consistent with the presence of a moderately strong expanding shock wave surrounding the radio lobes of 3C 444 at a distance of ~ 200 kpc from the cluster

centre. Further evidence for the presence of a shock comes from our spectral analysis: there is a temperature jump of a factor 1.7 ± 0.4 at the edge of the North lobe. Note that this temperature jump is likely to be an underestimate: the relatively low count levels from our short observation mean that large spectral extraction regions are required, which are likely to average over cooler regions further from the shock front. This temperature jump corresponds to a Mach number of 1.7 ± 0.4, confirming that a shock is indeed present. The Mach number calculated is significantly lower than that implied by the surface brightness jump, $\mathcal{M} \sim 3$. This may be because the temperature jump is underestimated due to averaging the hottest emission regions with cooler material further from the shock, or could be partly due to the geometrical and uniform density assumptions. The temperature structure around the South radio lobe is more ambiguous - the temperature appears higher in a region somewhat closer to the nucleus, and comparatively cool (~ 3 keV) at the outer edge. The reason for this is unclear, but could be due to significant asymmetry in the temperature distribution of the environment and perhaps some contribution from projection effects.

4. DYNAMICS AND ENERGETIC IMPACT OF 3C 444

To investigate further the source dynamics and energetic impact, we estimated the external pressure surrounding the outer radio lobes, and compared it with the internal radio lobe pressure under various assumptions. We estimated the external pressure acting on the radio lobes by considering the northern and southern quadrants of annuli 2 and 3, described above. We assumed each region had the geometry of an ellipsoidal shell (subtracting the overlapping volume of the radio lobe in each case) with a constant density contained within it and the mean temperature from the two spectral regions corresponding to each shell. Using the temperatures listed in Table 1, we determined densities of $n_{\rm p} = 0.047$ and 0.036 cm^{-3} for the northern and southern quadrants, respectively, which correspond to external pressures of $\sim 8.4 \times 10^{-12}$ Pa and $\sim 4.9 \times 10^{-12}$ Pa, respectively (we do not quote errors as the uncertainty is dominated by systematic error due to the geometrical assumptions and assumption of uniform density). The internal lobe pressures were determined under the assumption of no protons in three different scenarios: (1) equipartition between magnetic field and radiating particles, (2) a magnetic field strength $B = 0.7B_{\rm eq}$, the median found for FRII radio galaxies in the inverse-Compton study of Croston et al. (2005), and (3) the magnetic field strength leading to inverse-Compton emission just below the measured upper limit for the lobes of 9 nJy at 1 keV (see Section 2, above). These gave pressures for the North lobe of 3.6×10^{-13} Pa (scenario 1), 9×10^{-13} Pa (scenario 2), and 2.1×10^{-12} Pa (scenario 3), and for the South lobe of 2.3×10^{-13} Pa (scenario 1), 6.7×10^{-13} Pa (scenario 2), and 1.3×10^{-12} Pa (scenario 3). A comparison with the external pressure measured above ($P_{ext}/P_{int} \sim 14-23, 5-9$, and $4-6$, respectively, for the three scenarios above) demonstrates that the lobes would be underpressured in all of these scenarios, indicating that non-radiating particles (e.g. protons) are likely to dominate the lobe pressure. An apparent pressure imbalance of this sort is commonly found for low-power radio galaxies (e.g. Croston et al. 2008), but the good agreement with equipartition magnetic fields from inverse-Compton studies has previously been used to argue against a significant proton population in FRII radio galaxies (e.g. Croston et al. 2005). Environmental pressure comparisons for powerful FRII radio galaxies (e.g.

Croston et al. 2004; Belsole et al. 2007) indicate that in general the requirements for proton content are smaller than in FRI radio galaxies; however, FRII radio galaxies in the most rich environments appear more proton-dominated (Belsole et al. 2007; Hardcastle & Croston 2010). This supports the argument of Croston et al. (2008) that radio-galaxy particle content on large-scales is related to radio morphology, which can indicate the radio jets' ability to entrain material from the surroundings. The FRII radio galaxies in rich environments, like 3C 444, may therefore have a higher proton content than those in poorer environments (e.g. Croston et al. 2004).

The thermal proton density in the heated region immediately surrounding the northern lobe edge was also used to estimate the total energetic impact of the radio galaxy. Assuming that the material in this region has been heated from the measured pre-shock temperature of 3.6 keV, the total "excess" energy in the hot region is $\sim 8.2 \times 10^{60}$ ergs. If the lobes are assumed slightly overpressured (e.g. $\sim 1.5 \times P_{ext}$), consistent with the observed shock, then the work done by the Northern lobe is $1.5P_{ext}V \sim 1.4 \times 10^{60}$ ergs, a factor of ~ 6 lower than the required heating. Note that as we have ignored any heating in the E, W and S quadrants, the measured energy input could therefore be considered a lower limit. Finally, we used the measured energy input from the radio galaxy to estimate the jet power. We estimated the lobe inflation timescale by considering the sound crossing time, as well as the inflation time if the expansion was constant at the currently observed shock speed of $\mathcal{M} \sim 1.5$. The true evolution of the expansion speed cannot easily be estimated: the lobe pressure would have been higher at earlier times, but so would the external pressure closer to the cluster center. We determine a sound-crossing timescale of $t_{cs} = 1.8 \times 10^8$ years, implying a jet power of $P_{jet} \sim 1.4 \times 10^{45}$ erg s^{-1}. The $\mathcal{M} = 1.5$ timescale is 1.2×10^8 years, implying a jet power of $P_{jet} = 2.2 \times 10^{45}$ erg s^{-1}. The sound crossing time is a conservative upper limit to the source age, and our energy estimate is a lower limit due to considering only the work done by the North lobe, and so we consider the associated jet power a lower limit. The 1.4-GHz radio luminosity of 3C 444 is $L_{1.4GHz} = 3.3 \times 10^{26}$ W Hz^{-1}, and so our estimated mechanical power is consistent, within the scatter, with the relation of Bîrzan et al. (2008). We note that as far as we are aware this is only the second jet power estimate from X-ray environmental observations, after Cygnus A, for a radio galaxy that can be classed unambiguously as an FRII based on both radio morphology and luminosity. Our results are therefore important for constraining the poorly known high-luminosity end of the relation between jet power and radio luminosity.

5. CONCLUSIONS

We have identified a 200-kpc scale shock in the cluster environment of the radio galaxy 3C 444, based on a sharp surface brightness drop-off and significant temperature increases at the edges of the radio lobes. We infer that the radio galaxy has injected a total energy ~ 4 times more than the work done by the radio lobes assuming pressure balance, which implies that estimates of FRII radio galaxy energy input based simply on PdV work will be underestimates due to the role of shock heating. We estimate a total energy input from the expanding radio galaxy of 8.2×10^{60} ergs, which implies a jet power of $(1.4 - 2.2) \times 10^{45}$ erg s^{-1}. Finally, based on a comparison of the external pressure with the internal pressure under various assumptions, we conclude that a significant proton contribution to the internal pressure is required, which

is unexpected for an FRII galaxy given the good agreement of inverse-Compton measurements with the minimum energy condition for the population as a whole. However, we conclude that this is consistent with results for a handful of other powerful radio galaxies in rich environments, and suggests a strong role for environmental interactions in determining particle and energy content.

REFERENCES

Belsole, E., Worrall, D.M., Hardcastle, M.J., Croston, J.H. 2007, MNRAS, 381, 1109

Bîrzan, L., McNamara, B.R., Nulsen, P.E.J., Carilli, C.L., Wise, M.W. 2008, ApJ, 686, 859

Cavagnolo, K.W., Donahue, M., Voit, G.M., Sun, M. 2008, ApJ, 683, 107

Cavagnolo, K.W., Donahue, M., Voit, G.M., Sun, M. 2009, ApJS, 182, 12

Cavagnolo, K.W., McNamara, B.R., Nulsen, P.E.J., Carilli, C.L., Jones, C., Bîrzan, L. 2010, ApJ, 720, 1066

Croston, J.H., Birkinshaw, M., Hardcastle, M.J., Worrall, D.M. 2004, MNRAS, 353, 879

Croston, J.H., Hardcastle, M.J., Harris, D.E., Belsole, E., Birkinshaw, M., Worrall, D.M. 2005, ApJ, 626, 733

Croston, J.H., Kraft, R.P., Hardcastle, M.J. 2007, ApJ, 660, 191

Croston, J.H., Hardcastle, M.J., Birkinshaw, M., Worrall, D.M., Laing, R.A. 2008, MNRAS, 386, 1709

Croston, J.H., et al. 2009, MNRAS, 395, 1999

Dunn, R.J.H., Fabian, A.C. 2008, MNRAS, 385, 757

Fabian, A.C., Sanders, J.S., Allen, S.W., Crawford, C.S., Iwasawa, K., Johnstone, R.M., Schemidt, R.W., Taylor, G.B. 2003, MNRAS, 344, 43

Fanaroff, B.L., Riley, J.M. 1974, MNRAS, 167, 31

Forman, W.R. et al. 2007, ApJ, 665, 1057

Hardcastle, M.J., Birkinshaw, M., Worrall, D.M. 1998, MNRAS, 294, 615

Hardcastle, M.J., Croston, J.H. 2010, MNRAS, 404, 2018

Heinz, S., Reynolds, C.S., Begelman, M.C. 1998, ApJ, 501, 126

Kaiser, C.R., Alexander, P. 1997, MNRAS, 286, 215

Kataoka, J., Stawarz, L. 2005, ApJ, 622, 797

Kraft, R.P., Vazquez, S.E., Forman, W.R., Jones, C., Murray, S.S., Hardcastle, M.J., Worrall, D.M., Churazov, E. 2003, ApJ, 592, 129

Morganti, R., Killeen, N.E.B., Tadhunter, C.N. 1993, MNRAS, 263, 1023

Nulsen, P.E.J., McNamara, B.R., Wise, M.W., David, L.P. 2005, ApJ, 628, 629

Nulsen, P.E.J., Hambrick, D.C., McNamara, B.R., Rafferty, D., Bîrzan, L., Wise, M.W., David, L.P. 2005, ApJ, 625, 9

Rawlings, S., Jarvis, M.J. 2004, MNRAS, 355, 9

Scheuer, P.A.G. 1974, MNRAS, 166, 513

Smith, D.A., Wilson, A.S., Arnaud, K.A., Terashima, Y., Young, A.J. 2002, ApJ, 565, 195

Tadhunter, C.N., Morganti, R., di Serego-Alighieri, S., Fosbury, R.A.E., Danziger, I.J. 1993, MNRAS, 263, 999